Safe Tracking Control Strategy of Nonlinear Systems with Unknown Initial Tracking Condition: A Secure Boundary Protection Method Based on Prescribed Finite-time Control

Zou Songnan, Li Xiaohua, and Liu Yang, *IEEE, Member*

***Abstract*—A safe tracking control problem is investigated for a class of nonlinear systems with unknown initial tracking condition. The safe tracking control is independent of the initial tracking condition with the help of a novel output mapping. A secure boundary protection method (SBPM) based on prescribed finite-time control and a new prescribed finite-time performance function (PFTPF) is proposed. The SBPM can guarantee the safe operation of the system when the desired output violates the output constraint function. The method can ensure the system satisfies both the tracking control performance specified by the PFTPF and the actual output constraints. It can effectively handle the abrupt changes of actual output constraints. To solve the excessive control input jitter problem caused by the sudden changes of the output constraints, a bidirectional filtering smoothing mechanism (BFSM) is proposed. Finally, the effectiveness and superiority of the proposed method are verified by simulations.**

***Index Terms*—Safe tracking control, bidirectional filtering smoothing mechanism, prescribed finite-time control, secure boundary protection method, actual output constraint**

I. Introduction

In order to guarantee safe operation of nonlinear systems, the states of some actual systems need to satisfy the specific constraints. This problem has inspired the interest of many scholars, and there have been a lot of research results on the output constraint control [1-6]. The majority of output constraint control studies make the assumption that the desired trajectory always falls inside the output constraint. Nevertheless, during system operation, the output restriction in actuality could alter unpredictably. The desired trajectory might breach the output constraint as a result of the circumstances. Consequently, the conventional approach to output constraint, like the barrier Lyapunov function (BLF) method, is not relevant in this case. To address this problem, [7] designed a safe tracking scheme to ensure that the system output does not violate the output constraint by tracking a new desired trajectory redesigned according to the output constraint. References [8] and [9] further extended the approach in [7]. Nevertheless, in order to ascertain whether the output constraint might be broken at the subsequent sampling time, this approach must forecast the system output. However, in these publications, figuring out the intended trajectory is a somewhat involved task.

The control performance limitation is a significant concern for nonlinear systems, in addition to the physical boundary constraints. In [10], the prescribed performance control approach was initially put forward. By using a prescribed performance function, the approach may ensure that the systems perform as intended in both transient and steady-state scenarios. At present, there have been many similar performance functions. Especially, there is a kind of prescribed finite-time performance functions (PFTPFs) which can ensure the system to converge to a steady-state accuracy range within a settling time [11]. Nowadays, a large number of results on prescribed performance control have emerged [12-16]. However, the prescribed performance control method needs to know the initial condition of the constrained variable. The performance function must be designed according to the initial condition. The traditional prescribed performance control strategy cannot be applied in any other situation. The references [17-19] suggested ways that are independent of the beginning condition to tackle the problem. However, these techniques are unable to address both the real output limits and the tracking control performance at the same time.

According to the above analysis, this paper takes into account the safe tracking problem for a class of nonlinear systems with unknown initial tracking condition. A safe tracking controller is designed by adopting a newly proposed SBPM. This approach allows for the automatic adjustment of the secure boundary based on the actual output constraint. In contrast to the techniques in [7-9], the suggested method assumes that the real output constraint are saltatory and time-varying. The controller ensures the safety of the system even in the event that the desired output conflicts with the output restriction. A BFSM that may successfully lessen the significant control input jitter is proposed. In this study, the real output constraint and the tracking performance constraint are obtained simultaneously.

This is how the rest of the article is organized. Section 2 provides an overview of the system, includes preliminary information, and describes the specifics of the SBPM. The system's stability analysis and controller design are presented in Section 3. Section 4 displays the findings of the simulation research results. The conclusion is found in Section 5.

Manuscript received October 13, 2023; revised May 13, 2024.

This work was supported in part by Open Fund of State Key Laboratory of Automotive Simulation and Control in Jilin University (20210219).

Zou Songnan is a Postgraduate of School of Electronic and Information Engineering, University of Science and Technology Liaoning, Anshan, TX 114051, China (e-mail: zousongnan@163.com).

Li Xiaohua is a Professor of School of Electronic and Information Engineering, University of Science and Technology Liaoning, Anshan, TX 114051, China (e-mail: lixiaohua6412@163.com).

Liu Yang is a Distinguished Professor of College of Automation and Electronic Engineering, Qingdao University of Science and Technology, Qingdao, TX 266061, China (e-mail: liuyang0595@163.com).

II. Problem formulation and preliminaries

A. System description

Consider the following nonlinear system [6].

$$\begin{cases} \dot{x}_i = f_i(\bar{x}_i) + g_i(\bar{x}_i)x_{i+1}, \quad i = 1, 2, ..., n-1 \\ \dot{x}_n = f_n(\bar{x}_n) + g_n(\bar{x}_n)u, \\ y(t) = x_1(t) \end{cases} \tag{1}$$

where $\bar{x}_i = [x_1, ..., x_i]^{\mathrm{T}}$; $u \in \mathrm{R}$, $y \in \mathrm{R}$ are the system states, the control input and the system output, respectively. $f_i(\bar{x}_i), g_i(\bar{x}_i)$ $(i = 1, 2, ..., n)$ are the nonlinear unknown functions. The system's tracking control and constraint control issue is taken into account.

Assumption 1[12] It is known the sign of $g_i(\bar{x}_i)$, but not the function $g_i(\bar{x}_i)$. It is assumed, without losing generality, that $g_i(\bar{x}_i) > 0$, and that $\underline{g}_i$ is an unknown constant, so that

$$0 \leq \underline{g}_i < |g_i(\bar{x}_i)| < \infty, \forall x \in \Omega$$

Assumption 2[13] The expected output y_d and its derivatives $y_d^{(i)}$ are bounded for $i = 1, 2, ..., n$.

Designing a safe tracking controller with specified finite-time performance based on the SBPM is the control objective. When the desired output remains inside the real constraint bounds, the system output tracks the desired trajectory and satisfies the inequality, for all $t \geq T_p$, $-\phi(t) < x_1(t) - y_d(t) < \phi(t)$. On the other hand, when the intended path crosses the constraint boundary, the system output follows the secure boundary constraints and $\rho_2 \leq k_{down} < x_1 < k_{up} \leq \rho_1$ for all $t \geq T_p$.

B. Preliminaries

Definition 1[20] If a time-varying function $\phi(t)$ has the four properties:

1) $\phi(t)$ is a C^n function;
2) $\lim_{t\to T} \phi(t) = l$, when $t \geq T$, $\phi(t) = l$;
3) $\phi(t) > 0$;
4) $\dot{\phi}(t) \leq 0$.

Then $\phi(t)$ is a PFTPF. $l > 0$ is a design parameter, $T > 0$ represents the settling time. The function that follows is utilized as a PFTPF in this work.

$$\phi(t) = \begin{cases} \left(\frac{T-t}{T}\right)^q K + l, & 0 \leq t < T \\ l, & t \geq T \end{cases} \tag{2}$$

where the design parameters are $q \geq n+1$ and $K > 0$.

A RBFNN is used to estimate a continuous function $f(Z) \in \Omega : R^q \to R$

$$f(Z) = \theta^{*\mathrm{T}}\varphi(Z) + w(Z), Z \in \Omega_Z \subset R^q \tag{3}$$

here $\theta^* \in R^\kappa$ represents the vector of the ideal weights , $\kappa > 1$ represents the neural network node number, $w(Z)$ denotes the approximation error with $w(Z) \leq W$, $W > 0$ is an unknown constant, $Z \in \Omega_Z \subset R^q$ denotes the input vector, $\varphi(Z) = [\varphi_1(Z), \varphi_2(Z)..., \varphi_\kappa(Z)]^{\mathrm{T}} \in R^\kappa$ is the Gaussian basis function vector which is defined as

$$\varphi_i(Z) = \exp\left(-\frac{\|Z - \omega_i\|^2}{2\nu_i^2}\right), \quad i = 1, 2, \ldots, \kappa \tag{4}$$

where v_i is the width of the Gaussian function and $\omega_i = [\omega_{i1}, \omega_{i2}, ..., \omega_{iq}]$ is the receptive field center.

Lemma 1 [21] Denoting the neural network radial basis functions as $\varphi(\bar{x}_n) = [\varphi_1(\bar{x}_n), ..., \varphi_\kappa(\bar{x}_n)]^{\mathrm{T}}$ and the input vectors of the radial basis function neural network (RBFNN) as $\bar{x}_n = [x_1, ..., x_n]^{\mathrm{T}}$, we affirm that for the positive constants o and l satisfying $o \leq l$, The inequality listed below is met.

$$||\varphi(\bar{x}_l)||^2 \leq ||\varphi(\bar{x}_o)||^2 \tag{5}$$

C. Secure boundary protection method(SBPM)

We presume that $\rho_1(t)$ and $\rho_2(t)$ are the two output constraint functions. We usually assume that the desired output y_d falls within this range, satisfying $\rho_2(t) < y_d < \rho_1(t)$, for the system's output constraint, which is often expressed as $\rho_2(t) < x_1 < \rho_1(t)$. However, in real-world scenarios, a number of variables could cause the actual physical limitation border to abruptly alter. This sudden change may lead to a difference between the desired output y_d and the physical constraint, which could put the system's output in danger. We will examine the output constraint control problem in this subsection and offer an SBPM-based solution.

We consider the following output constraint functions for analysis in this context.

$$\rho_1(t) = \begin{cases} \rho_{11}(t), & t < T_A \\ \rho_{12}(t), & t \geq T_A \end{cases} \tag{6}$$

$$\rho_2(t) = \begin{cases} \rho_{21}(t), & t < T_B \\ \rho_{22}(t), & t \geq T_B \end{cases} \tag{7}$$

where the lower constraint is ρ_2 and the upper constraint is ρ_1. The smooth functions are $\rho_{11}, \rho_{12}, \rho_{21}, \rho_{22}$. T_A and T_B are the sudden changes moments in the constraints. The output must meet the next performance restriction in order to meet the control objective.

$$\bar{k}_{down}(t) < x_1(t) < \bar{k}_{up}(t), t \geq T_p \tag{8}$$

where the designable time parameter T_p and the desired boundaries are specified as

$$\bar{k}_{up}(t) = y_d(t) + \phi(t) \tag{9}$$

$$\bar{k}_{down}(t) = y_d(t) - \phi(t) \tag{10}$$

$\phi(t)$ is used to represent the PFTPF. the $x_1(t)$ will naturally be strictly constrained within the required bounds if inequality (8) is satisfied, and the PFTPF can accurately adjust the convergence rate. If the required limits are outside of the actual output restrictions, they will be adaptive adjusted to give two secure bounds. The secure boundaries will alter right away to prevent a violation of the output constraint since the bounds of the actual output constraint may change abruptly. Right now, the secure borders will yield an unsmooth point. The control input will jitter excessively as a result of this circumstance. This study proposes the BFSM method to suppress the high jitter in the control input and create smooth secure boundaries that do not stray from the planned trajectory.

It is well known that the filtered curve will get smoother when first-order filtering is used. Furthermore, when smoothness improves, filtering error will also rise. As a result, the BFSM is presented in this study.

Remark 1 Both inverse and conventional first-order filtering are referred to as bidirectional filtering in this context.

The function that needs to be filtered is referred to as the input in the former, and the filtered function along with its derivatives are the outputs. The exact reverse of the former is known as inverse filtering.

The BFSM operates on the following principle. To create the virtual security boundaries and virtual output constraints, the inverse filtering is first applied to the intended boundaries and actual output constraints. Then, the self-adjustment legislation (SAL), which is discussed later, ensures that the virtual output constraints are not broken by the virtual security barriers. Filtering forward the virtual secure borders finally yields the secure boundaries with upper and lower boundaries. The above-mentioned analysis shows that even though the virtual secure borders do not break the virtual output requirements, the secure boundaries will form the intended bounds if the forward and inverse filtering use the same filtering settings; when the virtual secure boundaries break the virtual output restrictions and the secure boundaries become smooth, the secure boundaries cannot also break the actual output constraint. The filtering parameter determines the degree of smoothness. Here is a description of the BFSM.

First, using inverse filtering, we create the subsequent virtual output limitations.

$$\hat{\rho}_1 = \begin{cases} \sigma\dot{\rho}_{11} + \rho_{11} = \hat{\rho}_{11}, & t < T_A \\ \sigma\dot{\rho}_{12} + \rho_{12} = \hat{\rho}_{12}, & t \geq T_A \end{cases} \tag{11}$$

$$\hat{\rho}_2 = \begin{cases} \sigma\dot{\rho}_{21} + \rho_{21} = \hat{\rho}_{21}, & t < T_B \\ \sigma\dot{\rho}_{22} + \rho_{22} = \hat{\rho}_{22}, & t \geq T_B \end{cases} \tag{12}$$

where the virtual output constraints are denoted by $\hat{\rho}_1, \hat{\rho}_2$, and σ is a filter constant. Next, the inverse filtering creates the subsequent virtual secure boundaries.

$$\hat{k}_{up} = \sigma\dot{\bar{k}}_{up} + \bar{k}_{up} \tag{13}$$

$$\hat{k}_{down} = \sigma\dot{\bar{k}}_{down} + \bar{k}_{down} \tag{14}$$

where the virtual secure boundaries are denoted by $\hat{k}_{up}$ and $\hat{k}_{down}$. The virtual secure boundaries by $\hat{\rho}_1, \hat{\rho}_2$ are checked with a SAL to make sure they don't go against the virtual output constraints. The virtual security borders can be forward filtered to acquire the genuine secure boundaries.

$$\dot{k}_{up} = \frac{\hat{k}_{up} - k_{up}}{\sigma} \tag{15}$$

$$\dot{k}_{down} = \frac{\hat{k}_{down} - k_{down}}{\sigma} \tag{16}$$

where the actual secure boundaries are k_{up}, k_{down}, $k_{up}, k_{down}, \dot{k}_{up}, \dot{k}_{down}$ can be created by (15), (16).

This is how the SAL is expressed. Only the situation where the upper constraint barrier is broken at T_A is taken into consideration for the sake of simplicity in explanation.

Case 1 $\hat{k}_{up}(T_A) \leq \hat{\rho}_1(T_A)$, $t \geq T_A$ is satisfied, the SAL is as follows.

$$\begin{aligned} & when \ \ \hat{k}_{up}(t) \geq \hat{\rho}_1(t) \\ & \begin{cases} \hat{k}_{up} = \hat{\rho}_1, \\ \hat{k}_{down} = \hat{\rho}_1 - 2\phi(t) \end{cases} \\ & else \\ & \begin{cases} \hat{k}_{up} = \hat{k}_{up}, \\ \hat{k}_{down} = \hat{k}_{down} \end{cases} \end{aligned} \tag{17}$$

Case 2 We consider the possibility that the system can learn about abrupt changes in the real physical boundaries before the t_m moment. When $t \geq T_A - t_m$, if the inequalities $\hat{k}_{up}(T_A - t_m) \leq \hat{\rho}_1(T_A)$, $\hat{k}_{up}(T_A) > \hat{\rho}_1(T_A)$ are fulfilled, one possesses

$$\begin{aligned} & when \ \ \hat{k}_{up}(t) \geq \hat{\rho}_{11}(t) \\ & \begin{cases} \hat{k}_{up} = \hat{\rho}_{11}, \\ \hat{k}_{down} = \hat{\rho}_{11} - 2\phi(t) \end{cases} \\ & else \\ & \begin{cases} \hat{k}_{up} = \hat{k}_{up}, \\ \hat{k}_{down} = \hat{k}_{down} \end{cases} \end{aligned} \tag{18}$$

Case 3 Unlike Cases 1 and 2, here the SAL must permit the k_{up} to return to the constraint range before to $t = T_A$ because when $t \geq T_A - t_m$, the following inequalities hold true: $\hat{k}_{up}(T_A - t_m) > \hat{\rho}_1(T_A)$, $\hat{k}_{up}(T_A) > \hat{\rho}_1(T_A)$.

In order to accomplish this, we establish $\tilde{k}_{up}(t) = \hat{k}_{up}(T_A - t_m) - \omega t$ and a function $\tilde{\rho}_{1i}(t)$. The search algorithm in Fig. 1 determines ω, $\tilde{\rho}_{1i}(t)$, which are used for the SAL. The search step sizes are ρ_m, ω_m, see Fig.1, and the positive design constants are $\omega_{\max}$, ω_0.

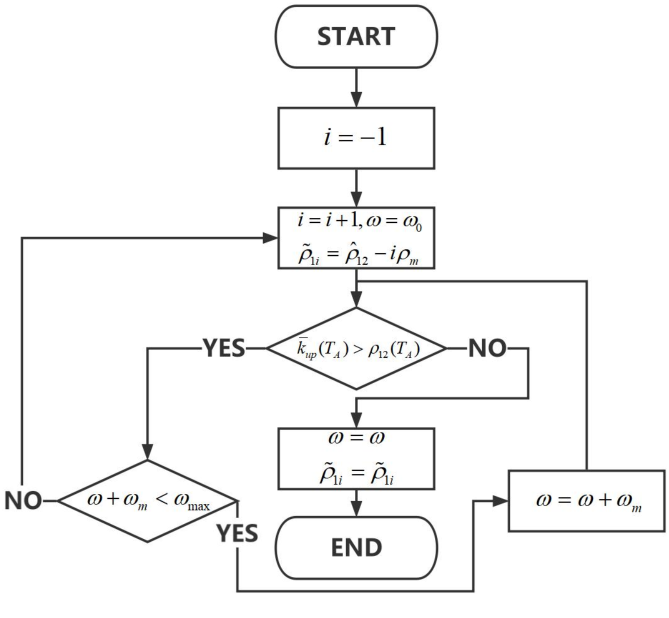

Fig.1. Selection process of $\tilde{\rho}_{1i}$ and ω

In Case 3, the $\hat{\rho}_1$ at T_A is smaller than the $\hat{k}_{up}$ at $T_A - t_m$., where the actual constraint boundary changes suddenly at T_A. This suggests that the virtual output constraint will be broken by the virtual secure border. At $T_A - t_m$. ω and $\tilde{\rho}_{1i}$ can be adjusted to guarantee that the $\hat{k}_{up}$ is always inside the $\hat{\rho}_1$. The search algorithm shown in Fig. 1 can help with this.

The SAL is as follows.

$$\begin{aligned} & when \ \ \tilde{k}_{up}(t) > \tilde{\rho}_{1i}(t), \, t < T_A \\ & \begin{cases} \hat{k}_{up} = \tilde{k}_{up}(t) = \hat{k}_{up}(T_A - t_m) - \omega t, \\ \hat{k}_{down} = \hat{k}_{up} - 2\phi(t) \end{cases} \\ & when \ \ \tilde{k}_{up}(t) \leq \tilde{\rho}_{1i}(t), t < T_A \\ & \begin{cases} \hat{k}_{up} = \tilde{\rho}_{1i}(t), \\ \hat{k}_{down} = \tilde{\rho}_{1i}(t) - 2\phi(t) \end{cases} \end{aligned}$$

$$
\begin{aligned}
&when \;\; \hat{k}_{up}(t) \geq \tilde{\rho}_{1i}(t), t \geq T_A \\
&\begin{cases} \hat{k}_{up} = \tilde{\rho}_{1i}(t), \\ \hat{k}_{down} = \tilde{\rho}_{1i}(t) - 2\phi(t) \end{cases} \\
&else \\
&\begin{cases} \hat{k}_{up} = \hat{k}_{up}, \\ \hat{k}_{down} = \hat{k}_{down} \end{cases}
\end{aligned} \tag{19}
$$

Remark 2 In SBPM, the three scenarios that violate the output constraints are taken into account. In Case 3, a virtual output boundary $\tilde{\rho}_{1i}$ is established, which can be changed with changes in the actual output constraints, to guarantee that the secure boundary is as smooth as possible and does not conflict with the real output boundary. Consequently, a smooth boundary curve can be produced, preventing the control signal from experiencing significant jitter.

Remark 3 We ought to select a lower value for the search phase. The created curve is better the smaller the value. However, calculations may get slower if the search step is too small. As a result, the smallest search step should be selected while maintaining computing speed as a prerequisite. An overly big parameter could prevent usable value from being obtained.

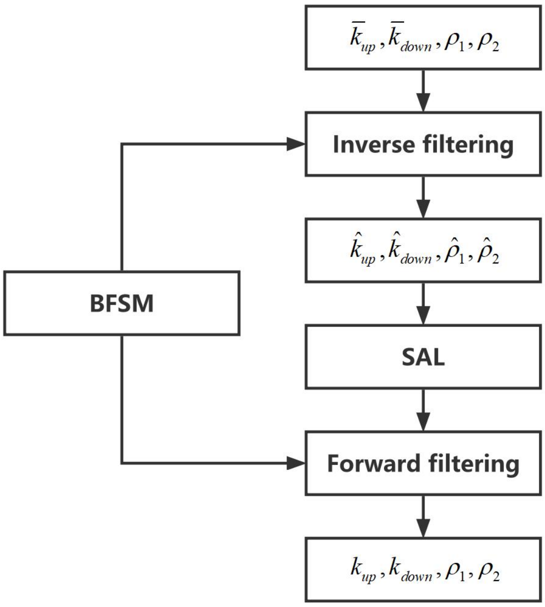

Fig.2. Implementation steps of the SBPM

A simulation demonstrating the efficacy of the BFSM is shown. Fig. 3 presents a effect of the BFSM, the secure boundary without filtering (SBWF), and the secure boundary with first order filter (SBWFOF). The secure boundary k_{up} has a smoothing effect, as shown by the comparison simulation results for the three approaches. Figure 3 shows that the suggested BFSM is able to smooth the secure border while also guaranteeing that it stays nearer to the y_d without breaking any of the constraints.

Remark 4 The study's suggested SBPM has the potential to manage the required performance as well as the output limitations. If the y_d does not clash with the actual output restrictions, the SBPM indicates that the system output meets $-\phi(t) < x_1(t) - y_d(t) < \phi(t), t \geq T_p$, which is according to the PFTPF. In the event that the y_d conflicts with the constraints, the secure boundary can ensure $k_{down} < x_1(t) < k_{up}$. Stated otherwise, the methodology outlined in this research is capable of simultaneously managing the output restrictions and the required performance.

Remark 5 The core methodology of this paper, SBPM, is a stand-alone design module that is independent of the system characteristics and control design methods. The method is able to handle systems with different characteristics such as unmodelled dynamics, unknown control direction, time lag, etc. and the scheme presented in this paper can be easily integrated with other control schemes.

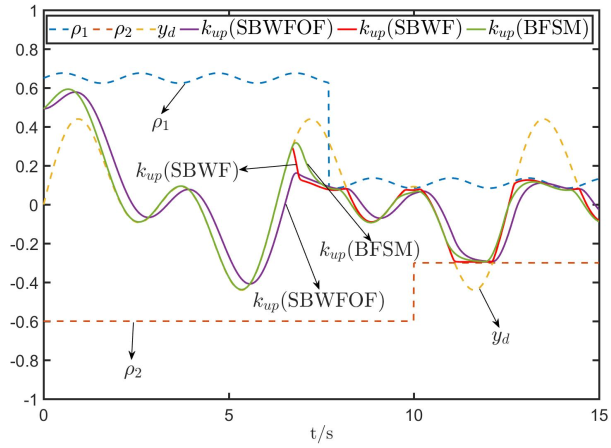

Fig.3. Secure boundaries created using various techniques

D. A novel output mapping

For the output $y(t)$, $k_{down}(0) < y(0) < k_{up}(0)$ must be met in traditional constraint control. However, in real-world applications, it's frequently challenging to collect the prerequisite beforehand. In this research, we offer a mapping function that allows the system to operate under any beginning condition while satisfying the output constraint and prescribed performance. We begin by defining a time-varying tuning function.

$$
\psi(t) = \begin{cases} \left(\frac{T_p - t}{T_p}\right)^r, & 0 \leq t < T_p \\ 0, & t \geq T_p \end{cases} \tag{20}
$$

where T_p is the point at which y enters the constraint range and $r \geq n+1$ represents a design constant. In this case, $\psi(t)$ represents a C^n function as well. Create the new mapping function that follows.

$$
z_1 = 0.5 \ln \frac{-k_{down}(1-\psi) + \psi(y^2 + k) + y}{k_{up}(1-\psi) + \psi(y^2 + k) - y} \tag{21}
$$

where $k \geq 1$ is a design parameter.

Remark 6 The approach in [17] can fulfill the constraint control under any initial state by applying a shifting function to zero the constrained variable. However, it must meet the requirements that $k_{up}(0) > 0$ and $k_{down}(0) < 0$, that is, The functions k_{down} and k_{up} have to be strictly positive or strictly negative. Unlike the approach in [17], k_{down} and k_{up} in (21) may reach the zero point and not always be positive or negative definite functions. There is a wider selection of constraint functions. Furthermore, $z_1(t) = 0.5 \ln \frac{(y(t)^2+k)+y(t)}{(y(t)^2+k)-y(t)}$ is clearly defined at $t = 0$ and is not affected by the values of k_{up}, k_{down}. This is also evident from (21). Consequently, there will be no requirement for the output's constraint initial condition. In addition, we may deduce from (21) that y is bounded if z_1 is bounded and satisfies $k_{down} < y < k_{up}$. Theorem 1 is provided in order to eloquently illustrate this concept.

Theorem 1 The resultant inequality holds irrespective of the $y(0)$ if z_1 is bounded, which implies that y is bounded as well.

$$k_{down} < y < k_{up}, \quad t \geq T_p \tag{22}$$

Proof: Observing that $k \geq 1$ and $\psi(0) = 1$, one obtains

$$\psi(0)(y^2(0) + k) > |y(0)| \tag{23}$$

From (21) and (23), one has

$$-k_{down}(0)(1 - \psi(0)) + \psi(0)(y^2(0) + k) + y(0) > 0 \tag{24}$$

$$k_{up}(0)(1 - \psi(0)) + \psi(0)(y^2(0) + k) - y(0) > 0 \tag{25}$$

Then we know $z_1(0)$ is well defined for any initial condition $y(0)$, then it is seen that $z_1 \to \infty$ if and only if $-k_{down}(1 - \psi) + \psi(y^2 + k) + y \to 0$ or $k_{up}(1 - \psi) + \psi(y^2 + k) - y \to 0$, therefore, if z_1 is bounded, it follows that

$$-k_{down}(1 - \psi) + \psi(y^2 + k) + y > 0 \tag{26}$$

$$k_{up}(1 - \psi) + \psi(y^2 + k) - y > 0 \tag{27}$$

Using (20), (26) and (27), one has $\psi = 0$ when $t \geq T_p$, one has

$$k_{down} < y < k_{up}, t \geq T_p \tag{28}$$

When $0 \leq t \leq T_p$, y can be derived as bounded by the continuity of y. ■

III. Controller design

First, by using the output mapping in (21), the performance constraint and the output constraints for $x_1(t)$ may be transformed

$$z_1 = 0.5 \ln \frac{-k_{down}(1 - \psi) + \psi(x_1^2 + k) + x_1}{k_{up}(1 - \psi) + \psi(x_1^2 + k) - x_1} \tag{29}$$

Create the coordinate transformations listed below.

$$z_i = x_i - \alpha_{i-1}, \quad i = 2, ..., n \tag{30}$$

where the virtual control law is denoted by α_{i-1}. The next first-order filter is shown in order to prevent differential explosion.

$$j_i \dot{\hat{\alpha}}_i + \hat{\alpha}_i = \alpha_i, \hat{\alpha}_i(0) = \alpha_i(0) \tag{31}$$

where j_i is a positive constant. Define the following filtering error

$$e_i = \alpha_i - \hat{\alpha}_i, i = 1, ..., n-1 \tag{32}$$

where $\hat{\alpha}_i$ is the output of the (31).

The real control law, the adaptive law, and the virtual control law are created as

$$\alpha_1 = -k_1 z_1 - z_1 - z_1 \hat{\eta}_1 \varphi_1^{\mathrm{T}} \varphi_1 \tag{33}$$

$$\alpha_i = -k_i z_i - z_i \hat{\eta}_i \varphi_i^{\mathrm{T}} \varphi_i - z_i - z_i \dot{\hat{\alpha}}_{i-1}^2 \tag{34}$$

$$u = -k_n z_n - z_n \hat{\eta}_n \varphi_n^{\mathrm{T}} \varphi_n - z_n - z_n \dot{\hat{\alpha}}_{n-1}^2 \tag{35}$$

$$\dot{\hat{\eta}}_1 = z_1^2 \varphi_1^{\mathrm{T}} \varphi_1 - \lambda_1 \hat{\eta}_1. \tag{36}$$

$$\dot{\hat{\eta}}_i = z_i^2 \varphi_i^{\mathrm{T}} \varphi_i - \lambda_i \hat{\eta}_i. \tag{37}$$

$$\dot{\hat{\eta}}_n = z_n^2 \varphi_n^{\mathrm{T}} \varphi_n - \lambda_n \hat{\eta}_n. \tag{38}$$

here $k_1, k_i, k_n > 0, \lambda_1, \lambda_i, \lambda_n > 0$ represent the control design constants, $\hat{\eta}_i$ represent the estimation parameter of $\eta_i^* = ||\theta_i^*||^2$, here $i = 1, ..., n$, the ideal vector of RBFNN, which is used to estimate continuous functions, is θ_i^*. The error of estimation is defined as

$$\tilde{\eta}_i = \hat{\eta}_i - \eta_i^*, \ i = 1, ..., n \tag{39}$$

Theorem 2 The closed-loop system satisfies the following conditions if the virtual control laws, actual control law, and adaptive laws for the system (1) with Assumptions 1∼2 are created in accordance with (33)∼(38): 1) The system's signals are all bounded; 2) If the desired output does not break the output requirements when $t \geq T_p$, then the tracking error can satisfy the required performance as given by the PFTPF; and 3) The inequality $\rho_2 < x_1 < \rho_1$ can be satisfied by the system output in cases when the desired trajectory deviates from the output constraints.

Proof: **Part 1**. Controller design

Step 1 From (29), we have

$$\begin{aligned} \dot{z}_1 =& \frac{\partial z_1}{\partial x_1}(f_1 + g_1 x_2) + \frac{\partial z_1}{\partial k_{down}} \dot{k}_{down} + \frac{\partial z_1}{\partial k_{up}} \dot{k}_{up} \\ &+ \frac{\partial z_1}{\partial \psi} \dot{\psi} \end{aligned} \tag{40}$$

Construct the following Lyapunov function

$$V_1 = \frac{1}{2} z_1^2 + \frac{1}{2} \tilde{\eta}_1^2 \tag{41}$$

From (41), one obtains

$$\dot{V}_1 = z_1(M_1(f_1 + g_1 x_2) + \beta_1) + \tilde{\eta}_1^{\mathrm{T}} \dot{\hat{\eta}}_1 \tag{42}$$

where

$$\begin{aligned} M_1 =& \frac{1}{2} \frac{2\psi x_1 + 1}{-k_{down}(1 - \psi) + \psi(x_1^2 + k) + x_1} \\ &- \frac{1}{2} \frac{2\psi x_1 - 1}{k_{up}(1 - \psi) + \psi(x_1^2 + k) - x_1} \end{aligned} \tag{43}$$

$$\begin{aligned} \beta_1 =& \frac{\partial z_1}{\partial k_{down}} \dot{k}_{down} + \frac{\partial z_1}{\partial k_{up}} \dot{k}_{up} + \frac{\partial z_1}{\partial \psi} \dot{\psi} \\ =& \frac{1}{2} [\frac{-1 + \psi}{-k_{down}(1 - \psi) + \psi(x_1^2 + k) + x_1}] \dot{k}_{down} \\ &- \frac{1}{2} [\frac{1 - \psi}{k_{up}(1 - \psi) + \psi(x_1^2 + k) - x_1}] \dot{k}_{up} \\ &+ \frac{1}{2} [\frac{k_{down} + x_1^2 + k}{-k_{down}(1 - \psi) + \psi(x_1^2 + k) + x_1} \\ &- \frac{-k_{up} + x_1^2 + k}{k_{up}(1 - \psi) + \psi(x_1^2 + k) - x_1}] \dot{\psi} \end{aligned} \tag{44}$$

From (30), one has

$$\begin{aligned} \dot{V}_1 =& z_1(M_1(f_1 + g_1 x_2) + \beta_1 - x_2 + z_2 + \alpha_1) \\ &+ \tilde{\eta}_1^{\mathrm{T}} \dot{\hat{\eta}}_1 \end{aligned} \tag{45}$$

Let $F_1 = M_1(f_1 + g_1x_2) + \beta_1 - x_2$, using an RBFNN to estimate F_1, we have

$$F_1 = \theta_1^{*\mathrm{T}}\varphi_1(Z_1) + w_1, w_1 < W_1 \tag{46}$$

here $Z_1 = [x, \psi, \dot{\psi}, k_{up}, \dot{k}_{up}, k_{down}, \dot{k}_{down}]$, $W_1 > 0$ is an unknown constant. From (46) and (45) we have

$$\dot{V}_1 \le z_1(\theta_1^{*\mathrm{T}}\varphi_1 + \alpha_1 + z_2) + |z_1W_1| + \tilde{\eta}_1^{\mathrm{T}}\dot{\hat{\eta}}_1 \tag{47}$$

Using Lemma 1 and Young's inequality, one has

$$|z_1W_1| \le \frac{W_1^2}{4} + z_1^2 \tag{48}$$

$$\begin{aligned} z_1\theta_1^{*\mathrm{T}}\varphi_1(Z_1) \le\ & |z_1|||\theta_1^*||||\varphi_1(X_1)|| \\ & \le z_1^2\eta_1^*\varphi_1(X_1)^{\mathrm{T}}\varphi_1(X_1) + \frac{1}{4} \end{aligned} \tag{49}$$

where $X_1 = [x_1, \psi, \dot{\psi}, k_{up}, \dot{k}_{up}, k_{down}, \dot{k}_{down}]$. Substituting (48), (49) into (47) gives

$$\begin{aligned} \dot{V}_1 \le & z_1(\alpha_1 + z_2) + z_1^2\hat{\eta}_1\varphi_1(X_1)^{\mathrm{T}}\varphi_1(X_1) + z_1^2 + \frac{W_1^2}{4} \\ & + \tilde{\eta}_1^{\mathrm{T}}(\dot{\hat{\eta}}_1 - z_1^2\varphi_1(X_1)^{\mathrm{T}}\varphi_1(X_1)) + \frac{1}{4} \end{aligned} \tag{50}$$

Substituting (33), (36) into (50) obtains

$$\begin{aligned} \dot{V}_1 \le & -k_1z_1^2 - \frac{\lambda_1}{2}\tilde{\eta}_1^2 + \frac{\lambda_1}{2}\eta_1^{*2} + \frac{W_1^2}{4} + \frac{1}{4} + z_1z_2 \\ \le & -\gamma_1V_1 + m_1 + z_1z_2 \end{aligned} \tag{51}$$

where $\gamma_1 = \min\{k_1, \frac{\lambda_1}{2}\}, m_1 = \frac{\lambda_1}{2}\eta_1^{*2} + \frac{W_1^2}{4} + \frac{1}{4}$.

Step i ($2 \le i \le n-1$) Let

$$V_i = V_{i-1} + \frac{1}{2}z_i^2 + \frac{\underline{g}_i}{2}\tilde{\eta}_i^2 + \frac{1}{2}e_{i-1}^2 \tag{52}$$

From (52), one has

$$\begin{aligned} \dot{V}_i \le & -\gamma_{i-1}V_{i-1} + m_{i-1} + z_i(f_i + g_{i-1}z_{i-1} - \dot{e}_{i-1} - \dot{\hat{\alpha}}_{i-1} \\ & + g_i\alpha_i + g_iz_{i+1}) + \underline{g}_i\tilde{\eta}_i^{\mathrm{T}}\dot{\hat{\eta}}_i + e_{i-1}\dot{e}_{i-1} \end{aligned} \tag{53}$$

where $\dot{e}_{i-1} = -\frac{e_{i-1}}{j_{i-1}} + \dot{\alpha}_{i-1}$. For the stated initial conditions [8], $\dot{\alpha}_{i-1}$ has a maximum B_{i-1} since $\dot{\alpha}_{i-1}$ represents a continue function on a compact set G_{i-1}.

Employing Young's inequality, one obtains

$$\begin{aligned} -z_i\dot{e}_{i-1} = & z_i(\frac{e_{i-1}}{j_{i-1}} - \dot{\alpha}_{i-1}) \\ & \le \frac{e_{i-1}^2}{4j_{i-1}} + \frac{(1+j_{i-1})z_i^2}{j_{i-1}} + \frac{1}{4}B_{i-1}^2 \end{aligned} \tag{54}$$

$$\begin{aligned} e_{i-1}\dot{e}_{i-1} \le & -\frac{e_{i-1}^2}{j_{i-1}} + |e_{i-1}\dot{\alpha}_{i-1}| \\ & \le -\frac{e_{i-1}^2}{j_{i-1}} + \frac{1}{2}e_{i-1}^2 + \frac{1}{2}B_{i-1}^2 \end{aligned} \tag{55}$$

Substituting (54), (55) into (53) gives

$$\begin{aligned} \dot{V}_i = & -\gamma_{i-1}V_{i-1} + m_{i-1} + z_i(f_i + g_{i-1}z_{i-1} + \frac{(1+j_{i-1})z_i}{j_{i-1}} \\ & - \dot{\hat{\alpha}}_{i-1} + g_i\alpha_i + g_iz_{i+1}) - (\frac{3}{4j_{i-1}} - \frac{1}{2})e_{i-1}^2 + \underline{g}_i\tilde{\eta}_i^{\mathrm{T}}\dot{\hat{\eta}}_i \\ & + \frac{3}{4}B_{i-1}^2 \end{aligned} \tag{56}$$

Define $F_i = f_i + \frac{(1+j_{i-1})z_i}{j_{i-1}} + g_{i-1}z_{i-1}$, we have.

$$F_i = \theta_i^{*\mathrm{T}}\varphi_i(Z_i) + w_i, w_i < W_i \tag{57}$$

here the constant $W_i > 0$ is unknown. Substituting (57) into (56) gives

$$\begin{aligned} \dot{V}_i = & -\gamma_{i-1}V_{i-1} + m_{i-1} + z_i({\theta_i}^{*\mathrm{T}}\varphi_i - \dot{\hat{\alpha}}_{i-1} + g_i\alpha_i \\ & + g_iz_{i+1}) + z_iW_i - (\frac{3}{4j_{i-1}} - \frac{1}{2})e_{i-1}^2 + \underline{g}_i\tilde{\eta}_i^{\mathrm{T}}\dot{\hat{\eta}}_i \\ & + \frac{3}{4}B_{i-1}^2 \end{aligned} \tag{58}$$

Employing Young's inequality, we arrive at

$$z_iW_i \le \frac{W_i^2}{4\underline{g}_i} + \underline{g}_iz_i^2 \tag{59}$$

$$z_i\theta_i^{*\mathrm{T}}\varphi_i(Z_i) \le \underline{g}_iz_i^2\eta_i^*\varphi_i(Z_i)^{\mathrm{T}}\varphi_i(Z_i) + \frac{1}{4\underline{g}_i} \tag{60}$$

Substituting (59), (60) into (58) gives

$$\begin{aligned} \dot{V}_i = & -\gamma_{i-1}V_{i-1} + m_{i-1} + z_i(-\dot{\hat{\alpha}}_{i-1} + g_i\alpha_i + g_iz_{i+1}) \\ & + \underline{g}_iz_i^2\hat{\eta}_i\varphi_i^{\mathrm{T}}\varphi_i + \underline{g}_iz_i^2 - (\frac{3}{4j_{i-1}} - \frac{1}{2})e_{i-1}^2 \\ & + \underline{g}_i\tilde{\eta}_i^{\mathrm{T}}(\dot{\hat{\eta}}_i - z_i^2\varphi_i^{\mathrm{T}}\varphi_i) + \frac{3}{4}B_{i-1}^2 + \frac{1}{4\underline{g}_i} + \frac{W_i^2}{4\underline{g}_i} \end{aligned} \tag{61}$$

When Young's inequality is combined with equation (34) it yields

$$z_ig_i\alpha_i \le -k_i\underline{g}_iz_i^2 - \underline{g}_iz_i^2\hat{\eta}_i\varphi_i^{\mathrm{T}}\varphi_i - \underline{g}_iz_i^2 - \underline{g}_iz_i^2\dot{\hat{\alpha}}_{i-1}^2 \tag{62}$$

$$-z_i\dot{\hat{\alpha}}_{i-1} \le \frac{1}{4\underline{g}_i} + \underline{g}_iz_i^2\dot{\hat{\alpha}}_{i-1}^2 \tag{63}$$

Substituting (37), (62), (63) into (61) has

$$\begin{aligned} \dot{V}_i \le & -\gamma_{i-1}V_{i-1} + m_{i-1} - k_i\underline{g}_iz_i^2 - \frac{\lambda_i}{2}\tilde{\eta}_i^{\mathrm{T}}\tilde{\eta}_i \\ & - (\frac{3}{4j_{i-1}} - \frac{1}{2})e_{i-1}^2 + \frac{\lambda_i}{2}\eta_i^{*\mathrm{T}}\eta_i^* + \frac{1}{4\underline{g}_i} + \frac{W_i^2}{4\underline{g}_i} \\ & + \frac{3}{4}B_{i-1}^2 + g_iz_iz_{i+1} \\ \le & -\gamma_iV_i + m_i + g_iz_iz_{i+1} \end{aligned} \tag{64}$$

where$\gamma_i = \min\left\{\gamma_{i-1}, k_i\underline{g}_i, \frac{\lambda_i}{2}, \frac{3}{4j_{i-1}} - \frac{1}{2}\right\}$,$m_i = m_{i-1} + \frac{\lambda_i}{2}\eta_i^{*\mathrm{T}}\eta_i^* + \frac{1}{4\underline{g}_i} + \frac{W_i^2}{4\underline{g}_i} + \frac{3}{4}B_i^2$.

Step n Let

$$V_n = V_{n-1} + \frac{1}{2}z_n^2 + \frac{\underline{g}_n}{2}\tilde{\eta}_n^2 + \frac{1}{2}e_{n-1}^2 \tag{65}$$

From (65), one has

$$\begin{aligned} \dot{V}_n \le & -\gamma_{n-1}V_{n-1} + m_{n-1} + z_n(f_n + g_{n-1}z_{n-1} - \dot{e}_{n-1} \\ & - \dot{\hat{\alpha}}_{n-1} + g_nu) + \underline{g}_n\tilde{\eta}_n^{\mathrm{T}}\dot{\hat{\eta}}_n + e_{n-1}\dot{e}_{n-1} \end{aligned} \tag{66}$$

where $\dot{e}_{n-1} = -\frac{e_{n-1}}{j_{n-1}} + \dot{\alpha}_{n-1}$. Same as step i, $\dot{\alpha}_{n-1}$ has a maximum B_{n-1}.

Using Young's inequality, one obtains

$$\begin{aligned} -z_n\dot{e}_{n-1} = & z_n(\frac{e_{n-1}}{j_{n-1}} - \dot{\alpha}_{n-1}) \\ & \le \frac{e_{n-1}^2}{4j_{n-1}} + \frac{(1+j_{n-1})z_n^2}{j_{n-1}} + \frac{1}{4}B_{n-1}^2 \end{aligned} \tag{67}$$

$$e_{n-1}\dot{e}_{n-1} \leq -\frac{e_{n-1}^2}{j_{n-1}} + |e_{n-1}\dot{\alpha}_{n-1}|$$
$$\leq -\frac{e_{n-1}^2}{j_{n-1}} + \frac{1}{2}e_{n-1}^2 + \frac{1}{2}B_{n-1}^2 \quad (68)$$

Substituting (67), (68) into (66) gives

$$\begin{aligned}\dot{V}_n =& -\gamma_{n-1}V_{n-1} + m_{n-1} + z_n(f_n + g_{n-1}z_{n-1} \\ &+ \frac{(1+j_{n-1})z_n}{j_{n-1}} - \dot{\hat{\alpha}}_{n-1} + g_n u) - (\frac{3}{4j_{n-1}} - \frac{1}{2})e_{n-1}^2 \\ &+ \underline{g}_n\tilde{\eta}_n^{\mathrm{T}}\dot{\hat{\eta}}_n + \frac{3}{4}B_{n-1}^2\end{aligned} \quad (69)$$

Define $F_n = f_n + \frac{(1+j_{n-1})z_n}{j_{n-1}} + g_{n-1}z_{n-1}$, combining RBFNN we have.

$$F_n = \theta_n^{*\mathrm{T}}\varphi_n(Z_n) + w_n, w_n < W_n \quad (70)$$

here the constant $W_i > 0$ is unknown. Substituting (70) into (69) gives

$$\begin{aligned}\dot{V}_n =& -\gamma_{n-1}V_{n-1} + m_{n-1} + z_n({\theta_n}^{*\mathrm{T}}\varphi_n - \dot{\hat{\alpha}}_{n-1} + g_n u) \\ &+ z_n W_n - (\frac{3}{4j_{n-1}} - \frac{1}{2})e_{n-1}^2 + \underline{g}_n\tilde{\eta}_n^{\mathrm{T}}\dot{\hat{\eta}}_n + \frac{3}{4}B_{n-1}^2\end{aligned} \quad (71)$$

Using Young's inequality, one has

$$z_n W_n \leq \frac{W_n^2}{4\underline{g}_n} + \underline{g}_n z_n^2 \quad (72)$$

$$z_n\theta_n^{*\mathrm{T}}\varphi_n(Z_n) \leq \underline{g}_n z_n^2\eta_n^*\varphi_n(Z_n)^{\mathrm{T}}\varphi_n(Z_n) + \frac{1}{4\underline{g}_n} \quad (73)$$

Substituting (72), (73) into (71) gets

$$\begin{aligned}\dot{V}_i =& -\gamma_{n-1}V_{n-1} + m_{n-1} + z_n(-\dot{\hat{\alpha}}_{n-1} + g_n u) \\ &+ \underline{g}_n z_n^2\hat{\eta}_n\varphi_n^{\mathrm{T}}\varphi_n + \underline{g}_n z_n^2 - (\frac{3}{4j_{n-1}} - \frac{1}{2})e_{n-1}^2 \\ &+ \underline{g}_n\tilde{\eta}_n^{\mathrm{T}}(\dot{\hat{\eta}}_n - z_n^2\varphi_n^{\mathrm{T}}\varphi_n) + \frac{3}{4}B_{n-1}^2 + \frac{1}{4\underline{g}_n} \\ &+ \frac{W_n^2}{4\underline{g}_n}\end{aligned} \quad (74)$$

When Young's inequality is combined with equation (35) it yields

$$\begin{aligned}z_n g_n u \leq& -k_n\underline{g}_n z_n^2 - \underline{g}_n z_n^2\hat{\eta}_n\varphi_n^{\mathrm{T}}\varphi_n - \underline{g}_n z_n^2 \\ &- \underline{g}_n z_n^2\dot{\hat{\alpha}}_{n-1}^2\end{aligned} \quad (75)$$

$$-z_n\dot{\hat{\alpha}}_{n-1} \leq \frac{1}{4\underline{g}_n} + \underline{g}_n z_n^2\dot{\hat{\alpha}}_{n-1}^2 \quad (76)$$

Substituting (38), (75), (76) into (74) has

$$\begin{aligned}\dot{V}_n \leq& -\gamma_{n-1}V_{n-1} + m_{n-1} - k_n\underline{g}_n z_n^2 - \frac{\lambda_n}{2}\tilde{\eta}_n^{\mathrm{T}}\tilde{\eta}_n \\ &- (\frac{3}{4j_{n-1}} - \frac{1}{2})e_{n-1}^2 + \frac{\lambda_n}{2}\eta_n^{*\mathrm{T}}\eta_n^* + \frac{1}{4\underline{g}_n} + \frac{W_n^2}{4\underline{g}_n} \\ &+ \frac{3}{4}B_{n-1}^2 \\ \leq& -\gamma_n V_n + m_n\end{aligned} \quad (77)$$

here $\gamma_n = \min\left\{\gamma_{n-1}, k_n\underline{g}_n, \frac{\lambda_n}{2}, \frac{3}{4j_{n-1}} - \frac{1}{2}\right\}$,$m_n = \frac{\lambda_n}{2}\eta_n^{*\mathrm{T}}\eta_n^* + \frac{1}{4\underline{g}_n} + \frac{W_n^2}{4\underline{g}_n} + \frac{3}{4}B_n^2 + m_{n-1}$.

Part 2.

1) Proof for the boundedness.

$z_i (1 \leq i \leq n)$ are bounded, by (77). The theorem 1 tells us that if z_1 is bounded, then the constraint $k_{down} < x_1 < k_{up}$, $t \geq T_p$, is fulfilled. So, it can be seen that x_1 is bounded for $t > 0$. Then, $\alpha_1, \hat{\eta}_1, x_2$ are bounded, thus, we obtain $x_3, ..., x_n$, $\alpha_2, ..., \alpha_{n-1}$, $\theta_2, ..., \theta_n$, u are bounded.

2) Proof for the tracking error's prescribed performance after T_p when the desired trajectory complies with the output constraints.

We may deduce that $k_{down} = \bar{k}_{down}$, $k_{up} = \bar{k}_{up}$ from (13)~(19), The following inequality is true if the desired output does not break the output restriction.

$$\bar{k}_{down}(t) < x_1(t) < \bar{k}_{up}(t), \ t \geq T_p \quad (78)$$

From (9), (10) one obtains

$$-\phi(t) < x_1(t) - y_d(t) < \phi(t), \quad t \geq T_p \quad (79)$$

This can result in the $x_1 - y_d$ satisfying the prescribed performance according to the PFTPF.

3) When y_d violates the constraint, prove that $\rho_2 < x_1 < \rho_1, t \geq T_p$ can be satisfied by the system output.

From (11)-(19), when $t \geq T_p$, one has $k_{up} \leq \rho_1$, $k_{down} \geq \rho_2$, combining the inequality $k_{down} < x_1 < k_{up}$ yields $\rho_2 \leq k_{down} < x_1 < k_{up} \leq \rho_1$. Thus the inequality $\rho_2 < x_1 < \rho_1$ holds. ∎

Remark 7 A smaller l can result in better tracking accuracy for the PFTPF parameters; a lower T value or an increase in q can result in a faster rate of convergence. A trade-off needs to be established because an excessive control performance will lead to a huge control input. The real smoothness of the secure boundaries depends on σ. Large jitter in the control input can be effectively suppressed with a high enough value of σ.

Remark 8 The following is a summary of the suggested method's design steps.

Step 1: In the PFTPF, set q, l, T, T_p, K.

Step 2: In the SBPM, select the values for σ, ρ_m, $\omega_m, \omega_{\max}$, and ω_0.

Step 3: Using the SBPM, create the k_{up}, k_{down}.

Step 4: For the virtual control laws α_i, control input u, and adaptive law $\dot{\hat{\eta}}_i$, use (33)~(38).

IV. Simulation Studies

Consider the following nonlinear system [17].

$$\begin{cases}\dot{x}_1 = x_2 \\ \dot{x}_2 = -9.8\sin(x_1) - 2x_2 + 2u\end{cases} \quad (80)$$

In this simulation, the system's safe tracking control is examined. ODE5 is the solver, and 0.0001 is the simulation step. The control parameters are chosen as $k_1 = 1$, $k_2 = 20$, $\sigma = 0.25$, $j_2 = 0.01$, $\lambda_1 = \lambda_2 = 100$, $T = 2.5$, $r = 3$, $q = 4$, $\rho_m = 0.01$, $l = 0.0025$, $\hat{\omega} = 1$, $K = 0.5$, $\omega_m = 1$. The initial conditions are given as $x_2(0) = 0$, $[\hat{\eta}_1(0), \hat{\eta}_2(0)]^{\mathrm{T}} = [0, 0]^{\mathrm{T}}$. The three possibilities will be taken into consideration in order to confirm the efficacy of the suggested strategy. Case 1 is $x_1(0) = -0.7$, Case 2 is $x_1(0) = 0.6$, Case 3 is $x_1(0) = -0.1$. The neural network $\hat{\theta}_1^{\mathrm{T}}\varphi_1$ contains 7^7 nodes, its centers are $\bar{\omega}_i (i = 1, ..., 7^7)$ evenly spaced in $[-3, 3]$, and width $\nu_1 = 1.1$. $\hat{\theta}_2^{\mathrm{T}}\varphi_2$ contains

7^8 nodes, centers $\bar{\omega}_i(i=1,...,7^8)$ evenly spaced in $[-3,3]$, and width $\nu_2=1.1$. The output constraint and the desired trajectory are as follows.

$$\rho_1=\begin{cases}0.9+0.026\sin(3t), & 0\le t<8\\ 0.4+0.026\sin(3t), & t\ge 8\end{cases} \tag{81}$$

$$\rho_2=\begin{cases}-0.9, & 0\le t<7\\ -0.6, & t\ge 7\end{cases} \tag{82}$$

$$y_d=0.8\sin(t) \tag{83}$$

The control method is simulated in accordance with Theorem 2's controller design, and the outcomes are displayed in Figs.4∼5. The tracking response is shown in Fig. 4, and the state x_2 is shown in Fig. 5.

It doesn't matter if the initial output falls inside the constraint boundary, as can be observed in Fig. 4, the system output can enter the safety range based on the required time T_p. The x_1 is limited to a preset neighborhood surrounding the y_d within the settling time T, provided that the expected output does not break the output constraints. Stated otherwise, it satisfies the required performance according to the PFTPF. The safety boundary will change to make sure that the x_1 fulfills the constraint when the desired output and the constraint clash. The boundedness of the state x_2 is shown in Fig. 5.

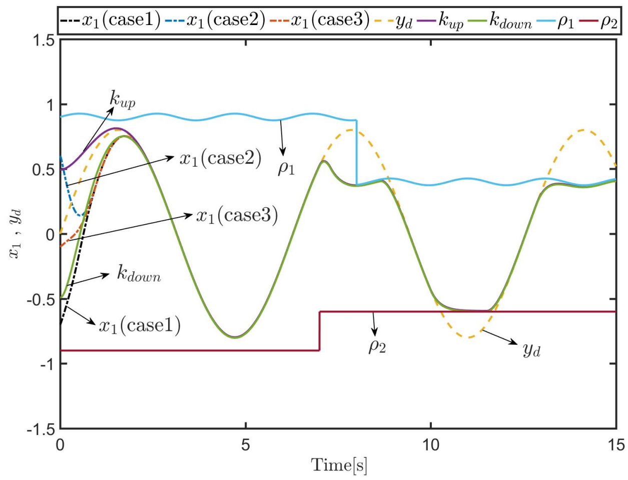

Fig.4. Tracking response

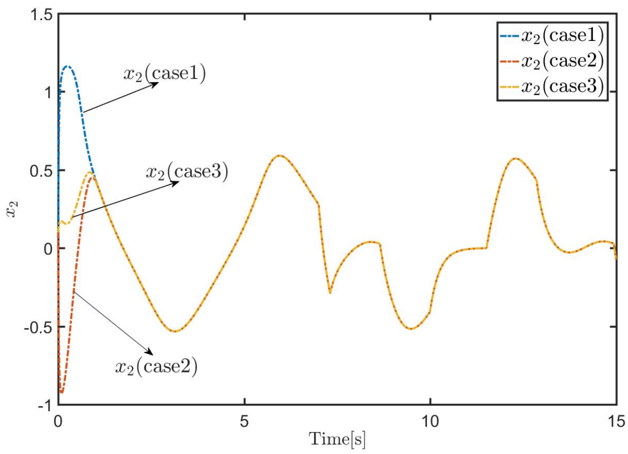

Fig.5. The system state x_2

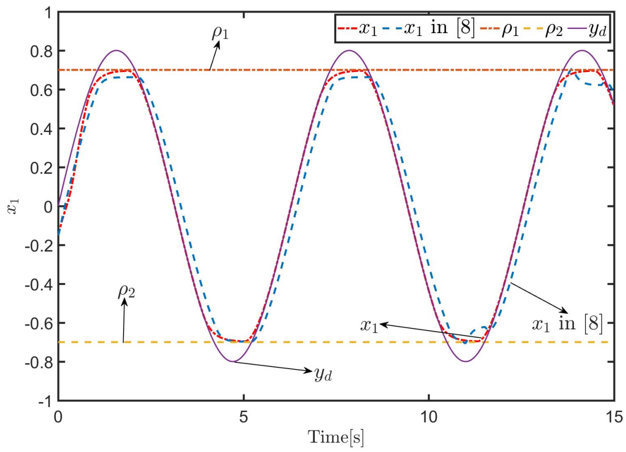

Fig.6. Safe tracking effect and comparison

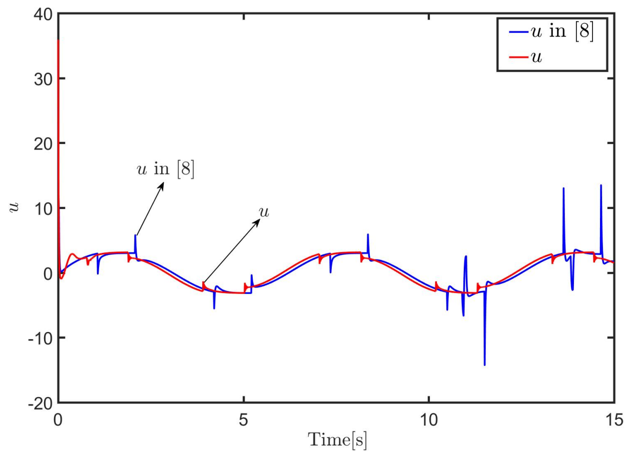

Fig.7. Control inputs and comparison

We compare with the procedure in [8] to confirm the superiority of the proposed method. In the simulation, the following parameters in [8] are consistent with this paper, they are $\rho_1=0.7$, $\rho_2=-0.7$, $y_d=0.8\sin(t)$, $k_1=5$, k_2 =25, $\lambda_1=\lambda_2=15$. The special parameters in the proposed method are set as $\sigma=0.25$, $T=2.5$, $j_2=0.01$, $r=3$, $q=4$, $l=0.0025$, ω_m= 1, $\hat{\omega}=1$, $K=0.5$, $\rho_m=0.01$. The special parameters in [8] are set as $\Delta t_s=0.01$, $\Delta t_{\min}=0.04$, $\Delta t_{\max}=0.2$, $c_{11}=c_{21}=-2$, $c_{12}=c_{22}=2$, which are the same as those in [8]. The initial conditions of the system are given as $x_1(0)=-0.15$, $x_2(0)=0$, $[\hat{\eta}_1(0),\hat{\eta}_2(0)]^{\mathrm{T}}=[0,0]^{\mathrm{T}}$. With the exception of the unique parameters in the two methods, all the parameters are the same. The simulation is shown in Fig.7 and Fig.8.

It is evident from the two figures that in situations where the planned trajectory clashes with the output constraints, the suggested technique performs safe tracking control. The approach in [8] can only guarantee that the system output does not exceed the output constraints to the best of its ability because its efficacy depends on the tracking control performance, parameter selection, and system output prediction. There is a lot of jittering in the control input, and if the control effect is pool, the strategy can be hazardous in practical situations. By using a batter tracking performance and smooth control input under the same control parameters, the strategy presented in this study is able to rigorously confine the output inside the output constraints; thus, the system's output curve is smoother than that of the method in [8]. Furthermore, it is important to highlight that the approach in [8] is not able to manage the time-varying and saltatory output requirements that are present in this study. That is, the output constraints considered in [8] are a special case of the constraints considered in this paper.

To further validate the effectiveness of this paper's scheme in more complex systems, the following third-order electromechanical system[11] is considered

$$\begin{cases} M\ddot{q} + B\dot{q} + N\sin q = I \\ V_0 - RI - K_B\dot{q} = L\dot{I} \end{cases} \tag{84}$$

here q represents the angular position, I is the armature current, V_0 represents the input control voltage. Let $x_1 = q$, $x_2 = \dot{q}$, $x_3 = I$, $u = V_0$, $y = x_1$, Add two items $\Lambda_1(\dot{q}, q, I)$ and $\Lambda_2(\dot{q}, q, I)$ based on [11].

$$\begin{cases} \dot{x}_1 = x_2 \\ \dot{x}_2 = \frac{1}{M}x_3 - \frac{N}{M}\sin x_1 - \frac{B}{M}x_2 + \Lambda_1(\dot{q}, q, I) \\ \dot{x}_3 = \frac{1}{L}u - \frac{K_B}{L}x_2 - \frac{R}{L}x_3 + \Lambda_2(\dot{q}, q, I) \\ y = x_1 \end{cases} \tag{85}$$

here $\Lambda_1(\dot{q}, q, I) = \frac{B}{M}x_2^2x_3^3$ and $\Lambda_2(\dot{q}, q, I) = \frac{R}{L}x_2^2\sin x_3$ representation the model error, $M = \frac{J}{K_\tau} + \frac{mL_0^2}{3K_\tau} + \frac{M_0L_0^2}{K_\tau} + \frac{2M_0R_0^2}{5K_\tau}$, $N = \frac{mL_0g}{2K_\tau} + \frac{M_0L_0g}{K_\tau}$, $B = \frac{B_0}{K_\tau}$. Here $J = 1.625 \times 10^{-3}kg \cdot m^2$, $M = 0.506kg$, $R_0 = 0.023m$, $M_0 = 0.434kg$, $L_0 = 0.305m$, $B_0 = 16.25 \times 10^{-3}N \cdot m \cdot s/rad$, $L = 25 \times 10^{-3}H$, $R = 5\Omega$, $K_\tau = K_B = 0.9N \cdot m/A$.

The initial conditions are $x_1(0) = 0.35$, $x_2(0) = 0$, $x_3(0) = 0$, $[\hat{\eta}_1(0), \hat{\eta}_2(0)], \hat{\eta}_3(0)]^{\mathrm{T}} = [0, 0, 0]^{\mathrm{T}}$. The controller is calculated according to Theorem 2. The simulation results are shown in Fig.8-Fig.9. Fig.8 represents the tracking response and Fig.9 represents the control input.

The simulation results demonstrate that, with the control method suggested in this study, the more complex third-order electromechanical system can still achieve a satisfactory control performance and complete the safe tracking control. Additionally, there is a noticeable suppression of the control input's considerable jitter.

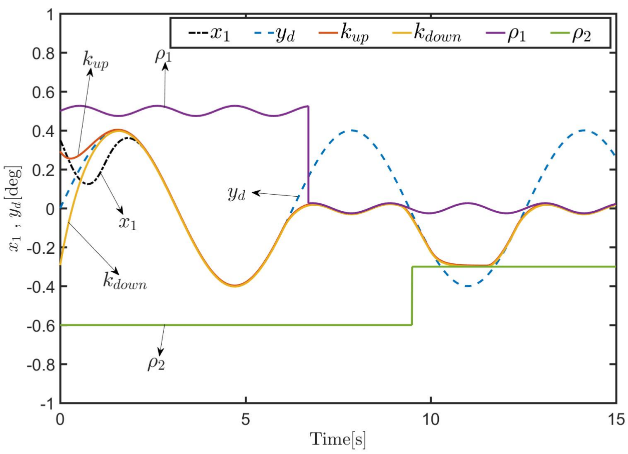

Fig.8. Tracking response

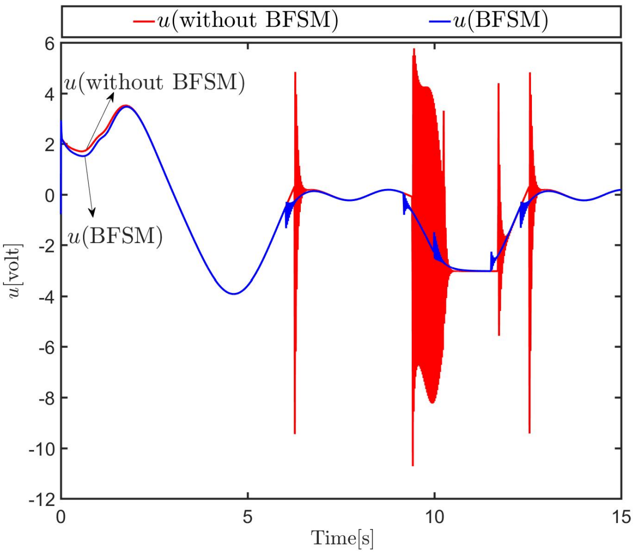

Fig.9. Control input and comparison

V. Conclusion

For a class of non-strict feedback nonlinear systems, This work suggests an finite-time initial tracking condition-free safe tracking control method. The three potential practical scenarios are examined, and an SBPM is provided to guarantee that the system output does not go against the output restriction. The SBPM takes into account both the output constraint and the prescribed performance at the same time. The desired trajectory can be adjusted without predicting the system output value, as the approach can handle abrupt changes in the actual output constraint with effectiveness. Additionally, by using the design parameters, the approach may be used to define the tracking accuracy and convergence speed. We suggest using the BFSM to smooth the secure boundary in order to mitigate the significant jitter in the control input while maintaining tracking performance. The suggested method's computing complexity is also much decreased at the same time. Significant application opportunities exist for the technique presented in this study in the domains of unmanned vehicle systems, UAVs, etc.

References

[1] Y. Liu, and Q. Zhu, "Adaptive neural network finite-time tracking control of full state constrained pure feedback stochastic nonlinear systems," *Journal of the Franklin Institute*, vol.357, no.11, pp.6738-6759, 2020.

[2] K. P. Tee, S. S. Ge, and E. H. Tay, "Barrier Lyapunov functions for the control of output-constrained nonlinear systems," *Automatica*, vol.45, no.4, pp.918-927, 2009.

[3] Y. Shang, and J. Huang, "Fixed-Time Stabilization of Spatial Constrained Wheeled Mobile Robot via Nonlinear Mapping." *IAENG International Journal of Applied Mathematics*, vol.50, no.4, pp.791-796, 2020.

[4] Z. Xu, N. Xie, H. Shen, X. Hu, and Q. Liu, "Extended state observer-based adaptive prescribed performance control for a class of nonlinear systems with full-state constraints and uncertainties," *Nonlinear Dynamics*, vol.105, no.1, pp.345-358, 2021.

[5] X. J. Xie, C. Guo, and R. H. Cui, "Removing feasibility conditions on tracking control of full-state constrained nonlinear systems with time-varying powers," *IEEE Transactions on Systems, Man, and Cybernetics: Systems*, vol.51, no.10, pp.6535-6543, 2020.

[6] Y. Shang, J. Huang, H. Li, and X. Wen,"Finite-Time Control Design for Nonholonomic Mobile Robots Subject to Spatial Constraint," *IAENG International Journal of Applied Mathematics*, vol.48, no.4, pp.449-454, 2018.

[7] S. Unnikrishnan, J. V. R. Prasad, and I. Yavrucuk, “Flight evaluation of a reactionary envelope protection system for UAVs,” *Journal of the American Helicopter Society*, vol.56, no.1, pp.12009-12009, 2011.
[8] M. Chen, H. Ma, Y. Kang, and Q. Wu, “Adaptive neural safe tracking control design for a class of uncertain nonlinear systems with output constraints and disturbances,” *IEEE Transactions on Cybernetics*, vol.52, no.11, pp.12571-12582, 2021.
[9] H. Ma, M. Chen, H. Yang, Q. Wu, and M. Chadli, “Switched safe tracking control design for unmanned autonomous helicopter with disturbances,” *Nonlinear Analysis: Hybrid Systems*, vol.39, no.100979, 2021.
[10] C. P. Bechlioulis, and G. A. Rovithakis, “Robust adaptive control of feedback linearizable MIMO nonlinear systems with prescribed performance,” *IEEE Transactions on Automatic Control*, vol.53, no.9, pp.2090-2099, 2008.
[11] Y. Liu, X. Liu, and Y. Jing, “Adaptive neural networks finite-time tracking control for non-strict feedback systems via prescribed performance,” *Information Sciences*, vol.468, pp.29-46, 2018.
[12] H. Liu, X. Li, and X. Liu, “A bounded-mapping-based prescribed constraint tracking control method without initial condition,” *Nonlinear Dynamics*, vol.111, no.4, pp.3451-3468, 2023.
[13] S. Zhou, X. Wang, and Y. Song, “Prescribed performance tracking control under uncertain initial conditions: a neuroadaptive output feedback approach,” *IEEE Transactions on Cybernetics*. 2022, 10.1109/TCYB.2022.3192356
[14] Y. Wang, J. Hu, J. Li, and B. Liu, “Improved prescribed performance control for nonaffine pure-feedback systems with input saturation,” *International Journal of Robust and Nonlinear Control*, vol.29, no.6, pp.1769-1788, 2019.
[15] K. Zhao, Y. Song, C. P. Chen, and L. Chen, “Adaptive asymptotic tracking with global performance for nonlinear systems with unknown control directions,” *IEEE Transactions on Automatic Control*, vol.67, no.3, pp.1566-1573, 2021.
[16] H. Wang, W. Bai, X. Zhao, and P. X. Liu, “Finite-time-prescribed performance-based adaptive fuzzy control for strict-feedback nonlinear systems with dynamic uncertainty and actuator faults,” *IEEE transactions on Cybernetics*, vol.52, no.7, pp.6959-6971, 2021.
[17] Y. D. Song, and S. Zhou, “Tracking control of uncertain nonlinear systems with deferred asymmetric time-varying full state constraints,” *Automatica*, vol.98, pp.314-322, 2018.
[18] H. Liu, and X. Li, “A prescribed-performance-based adaptive finite-time tracking control scheme circumventing the dependence on the system initial condition,” *Applied Mathematics and Computation*, vol.448, no.127912, 2023.
[19] J. X. Zhang, and G. H. Yang, “Robust adaptive fault-tolerant control for a class of unknown nonlinear systems,” *IEEE Transactions on Industrial Electronics*, vol.64, no.1, pp.585-594, 2016.
[20] S. Zou, X. Li, and Y. Liu. “Safe tracking control based on a secure boundary protection method for nonlinear systems with unknown initial tracking condition.” *International Journal of Systems Science*, pp.1-18, 2024.
[21] Y. Sun, B. Chen, C. Lin, H. Wang, and S. Zhou, “Adaptive neural control for a class of stochastic nonlinear systems by backstepping approach,” *Information Sciences*, vol.369, pp.748-764, 2016.